

Search for CP Violation in the Dalitz-Plot Analysis of

$$D^\pm \rightarrow K^+ K^- \pi^\pm$$

P. Rubin,¹ B. I. Eisenstein,² I. Karliner,² S. Mehrabyan,² N. Lowrey,² M. Selen,²
 E. J. White,² J. Wiss,² R. E. Mitchell,³ M. R. Shepherd,³ D. Besson,⁴ T. K. Pedlar,⁵
 D. Cronin-Hennessy,⁶ K. Y. Gao,⁶ J. Hietala,⁶ Y. Kubota,⁶ T. Klein,⁶ B. W. Lang,⁶
 R. Poling,⁶ A. W. Scott,⁶ P. Zweber,⁶ S. Dobbs,⁷ Z. Metreveli,⁷ K. K. Seth,⁷
 B. J. Y. Tan,⁷ A. Tomaradze,⁷ J. Libby,⁸ L. Martin,⁸ A. Powell,⁸ G. Wilkinson,⁸
 K. M. Ecklund,⁹ W. Love,¹⁰ V. Savinov,¹⁰ H. Mendez,¹¹ J. Y. Ge,¹² D. H. Miller,¹²
 I. P. J. Shipsey,¹² B. Xin,¹² G. S. Adams,¹³ D. Hu,¹³ B. Moziak,¹³ J. Napolitano,¹³ Q. He,¹⁴
 J. Insler,¹⁴ H. Muramatsu,¹⁴ C. S. Park,¹⁴ E. H. Thorndike,¹⁴ F. Yang,¹⁴ M. Artuso,¹⁵
 S. Blusk,¹⁵ S. Khalil,¹⁵ J. Li,¹⁵ R. Mountain,¹⁵ S. Nisar,¹⁵ K. Randrianarivony,¹⁵
 N. Sultana,¹⁵ T. Skwarnicki,¹⁵ S. Stone,¹⁵ J. C. Wang,¹⁵ L. M. Zhang,¹⁵
 G. Bonvicini,¹⁶ D. Cinabro,¹⁶ M. Dubrovin,¹⁶ A. Lincoln,¹⁶ P. Naik,¹⁷ J. Rademacker,¹⁷
 D. M. Asner,¹⁸ K. W. Edwards,¹⁸ J. Reed,¹⁸ R. A. Briere,¹⁹ G. Tatishvili,¹⁹
 H. Vogel,¹⁹ J. L. Rosner,²⁰ J. P. Alexander,²¹ D. G. Cassel,²¹ J. E. Duboscq*,²¹
 R. Ehrlich,²¹ L. Fields,²¹ L. Gibbons,²¹ R. Gray,²¹ S. W. Gray,²¹ D. L. Hartill,²¹
 B. K. Heltsley,²¹ D. Hertz,²¹ J. M. Hunt,²¹ J. Kandaswamy,²¹ D. L. Kreinick,²¹
 V. E. Kuznetsov,²¹ J. Ledoux,²¹ H. Mahlke-Krüger,²¹ D. Mohapatra,²¹ P. U. E. Onyisi,²¹
 J. R. Patterson,²¹ D. Peterson,²¹ D. Riley,²¹ A. Ryd,²¹ A. J. Sadoff,²¹ X. Shi,²¹
 S. Stroiney,²¹ W. M. Sun,²¹ T. Wilksen,²¹ S. B. Athar,²² R. Patel,²² and J. Yelton²²

(CLEO Collaboration)

¹George Mason University, Fairfax, Virginia 22030, USA

²University of Illinois, Urbana-Champaign, Illinois 61801, USA

³Indiana University, Bloomington, Indiana 47405, USA

⁴University of Kansas, Lawrence, Kansas 66045, USA

⁵Luther College, Decorah, Iowa 52101, USA

⁶University of Minnesota, Minneapolis, Minnesota 55455, USA

⁷Northwestern University, Evanston, Illinois 60208, USA

⁸University of Oxford, Oxford OX1 3RH, UK

⁹State University of New York at Buffalo, Buffalo, New York 14260, USA

¹⁰University of Pittsburgh, Pittsburgh, Pennsylvania 15260, USA

¹¹University of Puerto Rico, Mayaguez, Puerto Rico 00681

¹²Purdue University, West Lafayette, Indiana 47907, USA

¹³Rensselaer Polytechnic Institute, Troy, New York 12180, USA

¹⁴University of Rochester, Rochester, New York 14627, USA

¹⁵Syracuse University, Syracuse, New York 13244, USA

¹⁶Wayne State University, Detroit, Michigan 48202, USA

¹⁷University of Bristol, Bristol BS8 1TL, UK

¹⁸Carleton University, Ottawa, Ontario, Canada K1S 5B6

¹⁹Carnegie Mellon University, Pittsburgh, Pennsylvania 15213, USA

²⁰Enrico Fermi Institute, University of Chicago, Chicago, Illinois 60637, USA

* Deceased

²¹*Cornell University, Ithaca, New York 14853, USA*
²²*University of Florida, Gainesville, Florida 32611, USA*

Abstract

We report on a search for CP asymmetry in the singly Cabibbo-suppressed decay $D^+ \rightarrow K^+ K^- \pi^+$ using a data sample of 818 pb^{-1} accumulated with the CLEO-c detector on the $\psi(3770)$ resonance. A Dalitz-plot analysis is used to determine the amplitudes of the intermediate states. We find no evidence for CP violation either in specific two-body amplitudes or integrated over the entire phase space. The CP asymmetry in the latter case is measured to be $(-0.03 \pm 0.84 \pm 0.29)\%$.

PACS numbers: 13.25.Ft, 11.30.Er

D -meson decays are predicted in the Standard Model (SM) to exhibit CP -violating charge asymmetries smaller than $\mathcal{O}(10^{-3})$ [1]. Measurement of a CP asymmetry in the D system with higher rate would clearly signal new physics (NP) [2, 3]. Singly Cabibbo-suppressed (SCS) decays via $c \rightarrow u\bar{q}q$ transitions are sensitive to NP contributions to the $\Delta C = 1$ penguin process. Interestingly, such processes do not contribute to either the Cabibbo-favored ($c \rightarrow s\bar{d}u$) or the doubly Cabibbo-suppressed ($c \rightarrow d\bar{s}u$) decays. Direct CP violation in SCS decays could arise from interference between tree and penguin processes. A non-zero CP asymmetry can occur if there is both a strong and weak phase difference between the tree and penguin processes. In charged D -meson decays, mixing effects are absent, allowing us to probe direct CP violation and consequently NP.

Weak decays of D mesons are expected to be dominated by quasi two-body decays with resonant intermediate states. Dalitz-plot analysis techniques can be used to explore the resonant substructure. The intermediate structures of $D^+ \rightarrow K^+K^-\pi^+$ decay were studied by E687 [4] with a Dalitz-plot analysis and by FOCUS [5] with a non-parametric technique. *BABAR* searched for direct CP asymmetries in this mode using a counting method [6]. Using 281 pb $^{-1}$ of data, CLEO previously measured the absolute hadronic branching fractions and the CP asymmetries of Cabibbo-favored D -meson decay modes and the phase-space integrated asymmetry in the $K^+K^-\pi^+$ mode we study here [7]. The previous investigations of this decay were either limited by statistics, and did not search for CP violation, or did not study the resonant substructure.

We present the results of a search for direct CP asymmetry in the decay $D^\pm \rightarrow K^+K^-\pi^\pm$. This includes a study of the integrated decay rate, as well as decays through various intermediate states. We perform the present analysis on 818 pb $^{-1}$ of e^+e^- collision data collected at a center-of-mass energy of 3774 MeV with the CLEO-c detector [8, 9, 10] at the Cornell Electron Storage Ring (CESR). The CLEO-c detector is a general purpose solenoidal detector that includes a tracking system for measuring momentum and specific ionization (dE/dx) of charged particles, a Ring Imaging Cherenkov detector (RICH) to aid in particle identification, and a CsI calorimeter for detection of electromagnetic showers.

We reconstruct $D^+ \rightarrow K^+K^-\pi^+$, and the charge-conjugate mode $D^- \rightarrow K^+K^-\pi^-$. (Charge-conjugate modes are included throughout this report unless noted otherwise.) The event reconstruction criteria are the same as that used in Ref. [7]. Charged tracks are required to be well measured and to satisfy criteria based on the track fit quality. They must also be consistent with coming from the interaction point in three dimensions. Pions and kaons are identified using dE/dx and RICH information, when available. If either dE/dx or RICH information (or both) is missing we still use the track in the analysis. Detail can be found in Ref. [7]. We define two signal variables:

$$\Delta E \equiv \sum_i E_i - E_{\text{beam}} \quad (1)$$

and

$$m_{\text{BC}} \equiv \sqrt{E_{\text{beam}}^2 - \left| \sum_i \mathbf{p}_i \right|^2}, \quad (2)$$

where E_i and \mathbf{p}_i are the energy and momentum of each D decay product, and E_{beam} is the energy of one of the beams. For a correct combination of particles, ΔE should be consistent with zero, and m_{BC} should be consistent with the D^+ mass. Fig. 1 shows ΔE distribution of data. We select candidates that have ΔE within ± 12 MeV of zero, corresponding to 2.5 standard deviations (σ). If in any event there are multiple candidates satisfying the ΔE

criterion using entirely separate combinations of tracks, we accept all of these candidates. Otherwise if there are multiple candidates sharing tracks we keep only the combination with the smallest $|\Delta E|$.

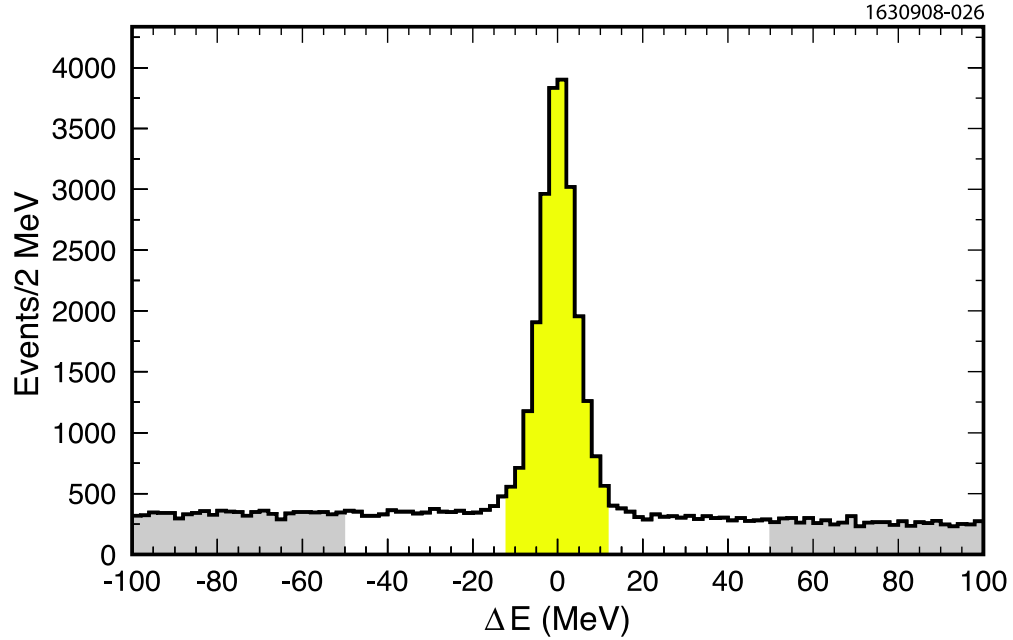


FIG. 1: The ΔE distributions. Signal ($|\Delta E| < 12$ MeV) and sidebands (50 MeV $< |\Delta E| < 100$ MeV) regions are shown.

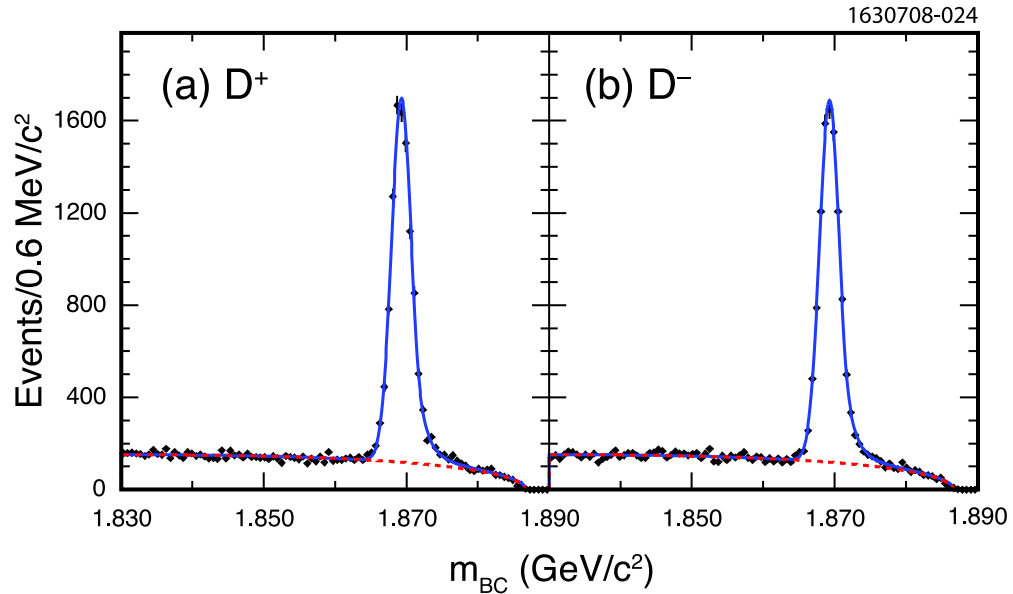


FIG. 2: The m_{BC} distributions for (a) D^+ and (b) D^- candidates. The solid curves show the fits to the data (points with error bars), while the dashed curves indicate the background.

To determine the signal yields of the D^+ and D^- samples, we simultaneously fit the m_{BC} distributions from the samples and require they have the same signal shape. For the signal,

we use a Crystal Ball line shape function [11], whose parameters are allowed to float. For the background, an ARGUS function [12] is used with shape parameters determined from the events in the ΔE sideband ($50 \text{ MeV} < |\Delta E| < 100 \text{ MeV}$). We find $9757 \pm 116 D^+$ and $9701 \pm 115 D^-$. Figure 2 shows the m_{BC} distributions of D^+ and D^- samples with fit functions superimposed; the total χ^2 is 241 for 180 degrees of freedom (d.o.f.).

We obtain the efficiency from a GEANT-based signal Monte Carlo (MC) simulation of the detector. The signal MC requires one of the two D mesons in an event to decay in accordance with all known modes and the other one to decay to the signal mode. For the signal D meson, we generate events that uniformly populate phase space. The average efficiency, accounting for a non-uniform population density of data, is calculated as follows. The Dalitz plot of the data is first divided into 16 bins that are approximately equally populated. The signal yields are obtained from the m_{BC} fits bin by bin and the corresponding efficiencies are calculated from the MC. The average efficiency is the sum of the yields divided by the sum of the efficiency-corrected yields. We find the efficiencies ϵ^\pm for the D^\pm decays are $(44.13 \pm 0.15)\%$ and $(43.85 \pm 0.15)\%$, respectively. The CP asymmetry, defined as

$$A_{CP} = \frac{N^+/\epsilon^+ - N^-/\epsilon^-}{N^+/\epsilon^+ + N^-/\epsilon^-}, \quad (3)$$

where N^\pm are the measured D^\pm yields, is measured as

$$A_{CP} = (-0.03 \pm 0.84 \pm 0.29)\% . \quad (4)$$

For the Dalitz-plot analysis, we consider the events from the signal box ($|\Delta E| < 12 \text{ MeV}$ and $|m_{\text{BC}} - m_{D^+}| < 4.5 \text{ MeV}/c^2$) corresponding to a 2.5σ range in each variable. The signal purity is $(84.26 \pm 0.10)\%$ obtained from the m_{BC} fit. The $K^+K^-\pi^+$ Dalitz-plot distribution is parameterized using the isobar model formalism described in Ref. [13]. The decay amplitude as a function of Dalitz-plot variables is expressed as a sum of two-body decay matrix elements,

$$\mathcal{M}(m_+^2, m_-^2) = \sum_r a_r e^{i\delta_r} \mathcal{A}_r(m_+^2, m_-^2), \quad (5)$$

where each term is parameterized with a magnitude a_r and a phase δ_r for the intermediate resonance r , and r ranges over all resonances. We choose $m_+^2 = m_{K^+\pi^+}^2$ and $m_-^2 = m_{K^-\pi^+}^2$ as the two independent Dalitz-plot variables. The partial amplitude $\mathcal{A}_r(m_+^2, m_-^2)$ is parameterized using the Breit-Wigner shape with Blatt-Weisskopf form factors in the D meson and intermediate resonance vertices [14], and angular dependence taken into account [13].

We use an unbinned maximum likelihood fit which maximizes the function

$$\mathcal{F} = \sum_{i=1}^N 2 \ln \mathcal{L}(m_{+,i}^2, m_{-,i}^2) - \left(\frac{f - f_0}{\sigma_f} \right)^2, \quad (6)$$

where the index i runs over all N events. The last term is used to constrain the signal fraction f to be the value f_0 within its error σ_f obtained from the m_{BC} fit. The first term contains the likelihood function

$$\mathcal{L}(m_+^2, m_-^2) = f \frac{\varepsilon(m_+^2, m_-^2) |\mathcal{M}|^2}{\mathcal{N}_{\text{sig}}} + (1 - f) \frac{F_{\text{bg}}(m_+^2, m_-^2)}{\mathcal{N}_{\text{bg}}}, \quad (7)$$

TABLE I: Fit results for three models with different S -wave parameterizations. The $K^-\pi^+$ S -wave contains contributions from $\overline{K}_0^*(1430)^0$ and a nonresonant term in fit A, from $\overline{K}_0^*(1430)^0$ and $\kappa(800)$ in fit B, and from the LASS amplitude in fit C. The errors are statistical, experimental systematic, and decay-model systematic, respectively.

	Magnitude	Phase ($^\circ$)	Fit Fraction (%)
Fit A [$\chi^2/\text{d.o.f.} = 898/708$]			
\overline{K}^{*0}	1(fixed)	0(fixed)	$25.0 \pm 0.6^{+0.4+0.2}_{-0.3-1.2}$
$\overline{K}_0^*(1430)^0$	$3.7 \pm 0.5^{+0.5+1.0}_{-0.1-1.0}$	$73 \pm 9^{+6+15}_{-6-38}$	$12.4 \pm 3.3^{+3.4+7.3}_{-0.7-5.8}$
ϕ	$1.189 \pm 0.015^{+0.000+0.028}_{-0.011-0.010}$	$-179 \pm 4^{+3+13}_{-1-5}$	$28.1 \pm 0.6^{+0.1+0.2}_{-0.3-0.4}$
$a_0(1450)^0$	$1.72 \pm 0.10^{+0.11+0.81}_{-0.11-0.28}$	$123 \pm 3^{+1+9}_{-1-15}$	$5.9 \pm 0.7^{+0.7+6.7}_{-0.6-1.8}$
$\phi(1680)$	$1.9 \pm 0.2^{+0.0+1.3}_{-0.1-0.7}$	$-52 \pm 8^{+0+10}_{-5-26}$	$0.51 \pm 0.11^{+0.02+0.85}_{-0.04-0.12}$
$\overline{K}_2^*(1430)^0$	$6.4 \pm 0.9^{+0.5+1.9}_{-0.4-3.6}$	$150 \pm 6^{+1+28}_{-0-13}$	$1.2 \pm 0.3^{+0.2+0.8}_{-0.1-0.6}$
NR	$5.1 \pm 0.3^{+0.0+0.6}_{-0.3-0.2}$	$53 \pm 7^{+1+18}_{-5-11}$	$14.7 \pm 1.8^{+0.2+3.9}_{-1.6-1.5}$
Total Fit Fraction = $(88.7 \pm 2.9)\%$			
Fit B [$\chi^2/\text{d.o.f.} = 895/708$]			
\overline{K}^{*0}	1(fixed)	0(fixed)	$25.7 \pm 0.5^{+0.4+0.1}_{-0.3-1.2}$
$\overline{K}_0^*(1430)^0$	$4.56 \pm 0.13^{+0.10+0.42}_{-0.01-0.39}$	$70 \pm 6^{+1+16}_{-6-23}$	$18.8 \pm 1.2^{+0.6+3.2}_{-0.1-3.4}$
ϕ	$1.166 \pm 0.015^{+0.001+0.025}_{-0.009-0.009}$	$-163 \pm 3^{+1+14}_{-1-5}$	$27.8 \pm 0.4^{+0.1+0.2}_{-0.3-0.4}$
$a_0(1450)^0$	$1.50 \pm 0.10^{+0.09+0.92}_{-0.06-0.33}$	$116 \pm 2^{+1+7}_{-1-14}$	$4.6 \pm 0.6^{+0.5+7.2}_{-0.3-1.8}$
$\phi(1680)$	$1.86 \pm 0.20^{+0.02+0.62}_{-0.08-0.77}$	$-112 \pm 6^{+3+19}_{-4-12}$	$0.51 \pm 0.11^{+0.01+0.37}_{-0.04-0.15}$
$\overline{K}_2^*(1430)^0$	$7.6 \pm 0.8^{+0.5+2.4}_{-0.6-4.8}$	$171 \pm 4^{+0+24}_{-2-11}$	$1.7 \pm 0.4^{+0.3+1.2}_{-0.2-0.7}$
$\kappa(800)$	$2.30 \pm 0.13^{+0.01+0.52}_{-0.11-0.29}$	$-87 \pm 6^{+2+15}_{-3-10}$	$7.0 \pm 0.8^{+0.0+3.5}_{-0.6-1.9}$
Total Fit Fraction = $(86.1 \pm 1.1)\%$			
Fit C [$\chi^2/\text{d.o.f.} = 912/710$]			
\overline{K}^{*0}	1(fixed)	0(fixed)	$25.3 \pm 0.5^{+0.2+0.2}_{-0.4-0.7}$
LASS	$3.81 \pm 0.06^{+0.05+0.13}_{-0.05-0.46}$	$25.1 \pm 2^{+1+6}_{-2-5}$	$40.6 \pm 0.8^{+0.4+1.6}_{-0.5-9.1}$
ϕ	$1.193 \pm 0.015^{+0.003+0.021}_{-0.010-0.011}$	$-176 \pm 2^{+0+8}_{-2-8}$	$28.6 \pm 0.4^{+0.2+0.2}_{-0.3-0.5}$
$a_0(1450)^0$	$1.73 \pm 0.07^{+0.14+0.68}_{-0.03-0.38}$	$122 \pm 2^{+1+8}_{-1-10}$	$6.0 \pm 0.4^{+0.9+5.5}_{-0.2-2.4}$
$\phi(1680)$	$1.71 \pm 0.16^{+0.02+0.41}_{-0.02-0.77}$	$-72 \pm 8^{+2+10}_{-2-22}$	$0.42 \pm 0.08^{+0.02+0.19}_{-0.01-0.16}$
$\overline{K}_2^*(1430)^0$	$4.9 \pm 0.7^{+0.1+2.2}_{-0.4-2.3}$	$146 \pm 9^{+0+34}_{-7-11}$	$0.7 \pm 0.2^{+0.0+0.7}_{-0.1-0.3}$
Total Fit Fraction = $(101.5 \pm 0.8)\%$			

where

$$\mathcal{N}_{\text{sig}} = \int \varepsilon(m_+^2, m_-^2) |\mathcal{M}|^2 dm_+^2 dm_-^2 \quad (8)$$

and

$$\mathcal{N}_{\text{bg}} = \int F_{\text{bg}}(m_+^2, m_-^2) dm_+^2 dm_-^2 \quad (9)$$

are the normalization factors, and $\varepsilon(m_+^2, m_-^2)$ and $F_{\text{bg}}(m_+^2, m_-^2)$ are efficiency and background functions. The fit parameters are a_r , ϕ_r and f .

We determine the efficiency $\varepsilon(m_+^2, m_-^2)$ using the same signal MC sample described before. The efficiency function is parameterized by a cubic polynomial in (m_+^2, m_-^2) multiplied by threshold factors $T(m_{+max}^2 - m_+^2; p_{xy}) \times T(m_{-max}^2 - m_-^2; p_{xy}) \times T(z_{max} - z; p_z)$, where

$$T(x; p) = \begin{cases} \sin(px) & , \quad 0 < px < \pi/2 \\ 1 & , \quad \text{otherwise} \end{cases} \quad (10)$$

$z \equiv m_{K^+K^-}^2$, m_{\pm}^2 or z_{max} is the maximum value of m_{\pm}^2 or z in this decay, p_{xy} and p_z are the fit parameters. The threshold factors are used to account for tracking inefficiency at the Dalitz-plot corners, where one of three particles might be produced with very low momentum and escape detection.

Figure 2 shows that the background is significant. To construct a model of the background shape $F_{bg}(m_+^2, m_-^2)$, we select events from the sideband region ($24 < |\Delta E| < 42$ MeV and $|m_{BC} - m_{D^+}| < 9$ MeV/ c^2). There are 12324 events, about 3.5 times the amount of background we estimate in the signal region, which is dominated by random combinations of unrelated tracks. Although the background includes ϕ and K^* mesons combined with random tracks, these events will not interfere with each other. Thus the shape is parameterized by a two-dimensional quadratic polynomial with terms representing non-coherent contributions from ϕ and K^* meson decays, multiplied by the threshold factors.

We consider fifteen intermediate states, $\phi\pi^+$, $\phi(1680)\pi^+$, $\bar{K}^{*0}K^+$, $\bar{K}_0^*(1430)^0K^+$, $\bar{K}^*(1410)^0K^+$, $\bar{K}_2^*(1430)^0K^+$, $\kappa(800)K^+$, $f_0(980)\pi^+$, $f_0(1370)\pi^+$, $f_0(1500)\pi^+$, $f_2(1270)\pi^+$, $f_2'(1525)\pi^+$, $a_0(980)^0\pi^+$, $a_0(1450)^0\pi^+$ and $a_2(1320)^0\pi^+$, as well as a nonresonant (NR) contribution. The parameters of the established resonances are taken from Ref. [15], except for the $f_0(980)$ which is taken from Ref. [16] and the $a_0(980)$ taken from Ref. [17]. A complex pole function is used to model the $\kappa(800)$ with pole position at $s_\kappa = (0.71 - i0.31)^2$ GeV² [18]. The nonresonant contribution is modeled as a uniform distribution over the allowed phase space. For the $K^-\pi^+$ S -wave states in the decays, we also consider the LASS amplitude as described in Ref. [19, 20], instead of a coherent sum of the states $\bar{K}_0^*(1430)^0K^+$, $\kappa(800)K^+$ and the nonresonant term.

This study is sensitive only to relative phases and magnitudes. The mode $\bar{K}^{*0}K^+$ is assigned to have zero phase and unit magnitude. We choose the same phase conventions for the intermediate resonances as E687 [4] used.

We begin to fit the data by considering only the three components \bar{K}^{*0} , ϕ , and $\bar{K}_0^*(1430)^0$ and obtain a result consistent with E687. To present a relative goodness-of-fit estimator, we divide the Dalitz-plot region into bins with dimensions 0.05 (GeV/ c^2)² \times 0.05 (GeV/ c^2)² and calculate χ^2 as

$$\chi^2 = -2 \sum_{i=1}^{721} n_i \ln \left(\frac{p_i}{n_i} \right), \quad (11)$$

where n_i (p_i) is the observed (expected) number of events in the i th bin [15]. We find $\chi^2 = 1292$ for $(721 - 5)$ d.o.f. in the ‘‘three resonances’’ fit, where 721 is the number of valid bins inside the kinematically allowed region.

Our twenty times larger statistics than E687 require a better model. We determine which additional resonances to include by the following procedure: starting from the three resonances and adding new resonances one at a time, we choose the best additional one at each iteration, stopping when no additional resonances have fit fractions (FF) more than 3σ from zero. The fit fraction is defined as

$$\text{FF}_r = \frac{\int |a_r \mathcal{A}_r|^2 dm_+^2 dm_-^2}{\int |\mathcal{M}|^2 dm_+^2 dm_-^2}. \quad (12)$$

The results of our fits are presented in Table I. We find that three fits (denoted as A-C) describe the data with similar quality. The only difference among them is in description of the $K^-\pi^+$ S -wave contribution, which is represented by the $\bar{K}_0^*(1430)^0$ and NR in fit A,

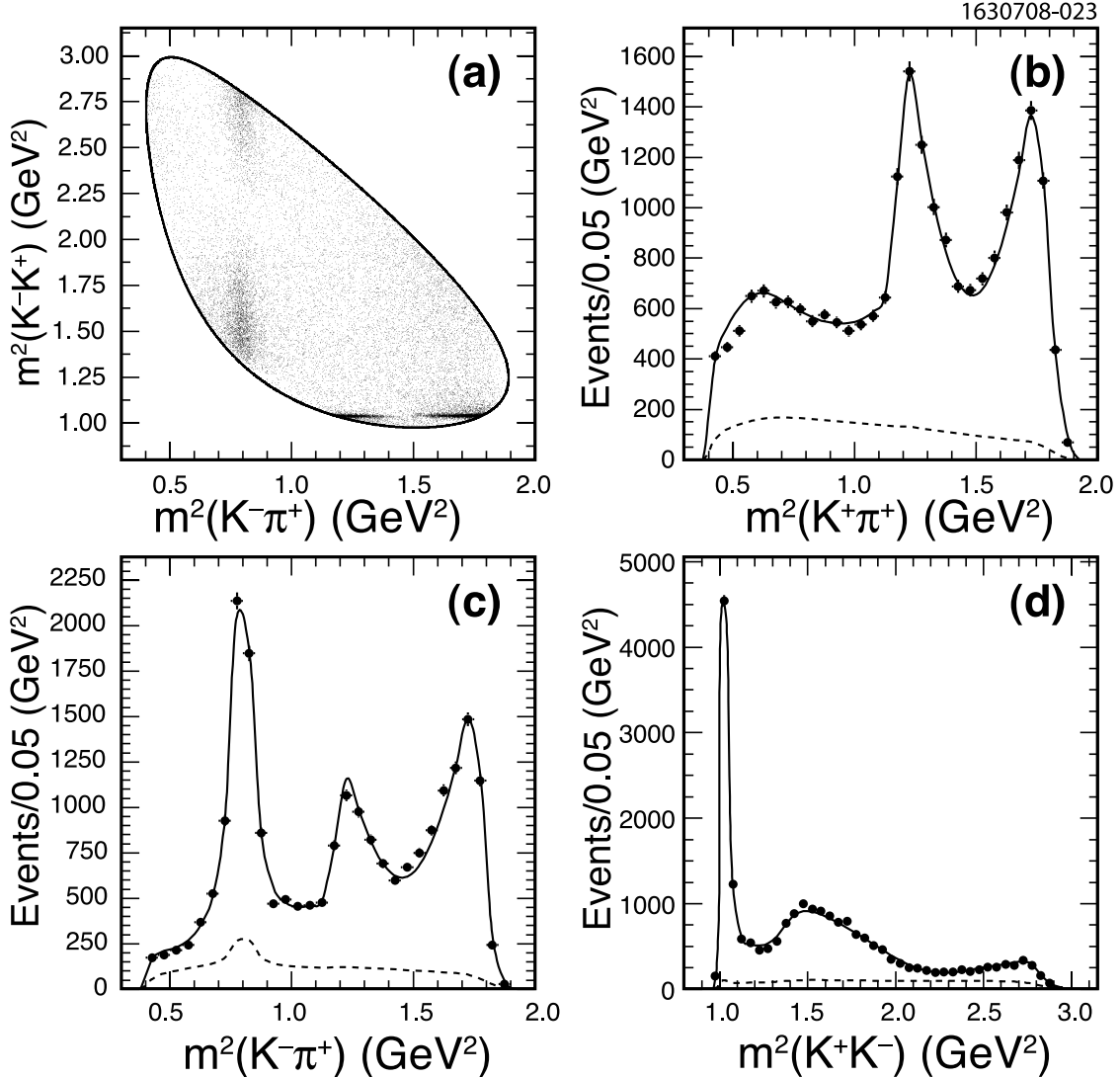


FIG. 3: (a) The Dalitz plot for $D^+ \rightarrow K^+K^-\pi^+$ candidates. (b)-(d) Projections of the results of the fit B (line) and the data (points). The dashed line shows the background contribution.

by $\overline{K}_0^*(1430)^0$ and $\kappa(800)$ in fit B, and by the LASS amplitude in fit C. Figure 3 shows the Dalitz plot for the $D^+ \rightarrow K^+K^-\pi^+$ candidates and three projections of the data with the result of fit B superimposed.

We generate seven sets of GEANT-based signal MC samples with the model from fit A. Each set contains about the same size as in the data. We find that the fits can recover the input magnitudes and phases within their errors.

Fit B gives the best agreement with the data; thus we choose it to search for CP -violation (CPV). The resonances in D^+ (D^-) decays are allowed to have different magnitudes, $a_r + b_r$ ($a_r - b_r$), and phases, $\delta_r + \phi_r$ ($\delta_r - \phi_r$), in the decay amplitude \mathcal{M} ($\overline{\mathcal{M}}$). We perform a simultaneous fit to D^+ and D^- samples. In the fit, the signal term in Eq. (7) is replaced by

$$\mathcal{L}_{\text{sig}} = \frac{f\varepsilon^+(m_+^2, m_-^2)|\mathcal{M}|^2}{\int \varepsilon^+(m_+^2, m_-^2)|\mathcal{M}|^2 dm_+^2 dm_-^2} \quad (13)$$

for the D^+ sample and by

$$\bar{\mathcal{L}}_{\text{sig}} = \frac{f \varepsilon^-(m_+^2, m_-^2) |\overline{\mathcal{M}}|^2}{\int \varepsilon^-(m_+^2, m_-^2) |\overline{\mathcal{M}}|^2 dm_+^2 dm_-^2} \quad (14)$$

for the D^- sample, where ε^\pm are efficiency functions obtained from the D^\pm signal MC separately. We cannot determine the relative magnitude and phase between D^+ and D^- directly, and assume $b = 0$ and $\phi = 0$ for the \overline{K}^{*0} resonance. The free parameters in the fit are b_r/a_r , a_r , δ_r , ϕ_r and f .

Following Ref. [21], we also compute the CP -conserving fit fraction as

$$\text{FF}(CPC)_r = \frac{\int |2a_r \mathcal{A}_r|^2 dm_+^2 dm_-^2}{\int (|\mathcal{M}|^2 + |\overline{\mathcal{M}}|^2) dm_+^2 dm_-^2}, \quad (15)$$

the CPV fit fraction as

$$\text{FF}(CPV)_r = \frac{\int |2b_r \mathcal{A}_r|^2 dm_+^2 dm_-^2}{\int (|\mathcal{M}|^2 + |\overline{\mathcal{M}}|^2) dm_+^2 dm_-^2}, \quad (16)$$

and the CPV interference fraction (IF) as

$$\text{IF}_r = \frac{\left| \int \sum_{k \neq r} [2a_k e^{i\delta_k} \cos(\phi_k - \phi_r) \mathcal{A}_k] b_r \mathcal{A}_r^* dm_+^2 dm_-^2 \right|}{\int (|\mathcal{M}|^2 + |\overline{\mathcal{M}}|^2) dm_+^2 dm_-^2}. \quad (17)$$

The CP -conserving fit fraction is the same for the D^+ and D^- by construction. The CPV fit fraction defined by Eq. (16) is sensitive to CP violation in the resonant decay. The CPV interference fractions of Eq. (17) sum over the contribution proportional to $a_k e^{+i\delta_k} b_r$ so they are sensitive to CP violation in interference between resonances. The phases are important and allow the possibility of cancelation in this sum.

In Table II, we report the magnitude asymmetries b_r/a_r , phase differences ϕ_r and fit fraction asymmetries. The fit fraction asymmetry is computed as the difference between the D^+ and D^- fit fractions divided by the sum. The largest fit fraction asymmetry, for the $\overline{K}_2^*(1430)^0$, is 1.7σ , and occurs because the fit fraction for the $\overline{K}_2^*(1430)^0$ is small. The CP -conserving fit fractions and the 95% confidence level (C.L.) upper limits for CPV fit fraction, CPV interference fraction, and the ratio of CPV interference to CP -conserving fit fraction are given in Table III. We notice that the CP -conserving fit fractions are consistent with those of fit B in Table I. Figure 4 shows the difference of the Dalitz-plot projections of data and fit between D^+ and D^- decays.

We calculate an integrated CP asymmetry across the Dalitz plot, defined as

$$\mathcal{A}_{CP} = \int \frac{|\mathcal{M}|^2 - |\overline{\mathcal{M}}|^2}{|\mathcal{M}|^2 + |\overline{\mathcal{M}}|^2} dm_+^2 dm_-^2 / \int dm_+^2 dm_-^2. \quad (18)$$

We obtain $\mathcal{A}_{CP} = (-0.4 \pm 2.0_{-0.5}^{+0.2+0.6})\%$, where the errors are statistical, experimental systematic, and decay-model systematic, respectively.

Using the same counting technique as in Ref. [6], we examine CP asymmetries (\mathcal{A}_{CP}) in the ϕ and \overline{K}^{*0} regions by requiring the K^+K^- and $K^-\pi^+$ invariant mass to be within 15

TABLE II: The magnitude asymmetries b_r/a_r , phase differences ϕ_r and asymmetries on the D^+ and D^- fit fractions from fit B. The errors are statistical, experimental systematic, and decay-model systematic, respectively.

r	b/a (%)	ϕ ($^\circ$)	FF asymmetry(%)
\overline{K}^{*0}	0(fixed)	0(fixed)	$-0.4 \pm 2.0^{+0.2+0.6}_{-0.5-0.3}$
$\overline{K}_0^*(1430)^0$	$4 \pm 3^{+1+2}_{-0-1}$	$-1 \pm 6^{+0+6}_{-3-1}$	$8 \pm 6^{+1+4}_{-1-1}$
ϕ	$-0.7 \pm 1.3^{+0.2+0.3}_{-0.1-0.2}$	$3 \pm 3^{+0+3}_{-1-1}$	$-1.8 \pm 1.6^{+0.0+0.2}_{-0.4-0.1}$
$a_0(1450)^0$	$-10 \pm 7 \pm 2^{+6}_{-3}$	$4 \pm 3^{+1+2}_{-2-1}$	$-19 \pm 12^{+5+6}_{-3-11}$
$\phi(1680)$	$-4 \pm 11^{+5+6}_{-4-4}$	$3 \pm 6 \pm 2^{+3}_{-2}$	$-9 \pm 22^{+10+9}_{-7-12}$
$\overline{K}_2^*(1430)^0$	$23^{+12+1+3}_{-11-7-7}$	5^{+5+1+3}_{-4-3-1}	$43 \pm 19^{+1+5}_{-13-12}$
$\kappa(800)$	$-6 \pm 6^{+3+1}_{-1-5}$	$3 \pm 6^{+4+1}_{-2-4}$	$-12 \pm 11^{+0+14}_{-6-2}$

TABLE III: The CP -conserving fit fractions from Eq. (15) and the 95% confidence level (C.L.) upper limits for CPV fit fraction from Eq. (16), CPV interference fraction from Eq. (17), and the ratio of CPV interference to CP -conserving fit fraction. The 95% C.L. upper limits include statistical and systematic effects.

Component	FF(CPC)(%)	FF(CPV) ($\times 10^{-3}$) (95% C.L. upper limits)	IF ($\times 10^{-3}$)	Ratio (%)
\overline{K}^{*0}	25.7 ± 0.5	0(fixed)	0(fixed)	0(fixed)
$\overline{K}_0^*(1430)^0$	18.8 ± 1.2	< 4.3	< 12.6	< 8.5
ϕ	27.8 ± 0.4	< 0.6	< 0.5	< 0.17
$a_0(1450)^0$	4.7 ± 0.6	< 10.8	< 31.6	< 45
$\phi(1680)$	0.50 ± 0.11	< 0.9	< 4.6	< 89
$\overline{K}_2^*(1430)^0$	1.8 ± 0.4	< 6.9	< 3.9	< 22
$\kappa(800)$	7.0 ± 0.8	< 4.2	< 17.2	< 25

and 10 MeV/ c^2 of the nominal ϕ and \overline{K}^{*0} masses [15]. We find A_{CP} ($-0.9 \pm 1.4 \pm 0.7$)% and ($0.3 \pm 1.8 \pm 0.6$)% for the ϕ and \overline{K}^{*0} region, respectively.

Systematic uncertainties from experimental sources and from the decay model are considered separately. Our general procedure is to change some aspect of our fit and interpret the change in the values of the magnitudes, phases, fit fractions, b_r/a_r , ϕ_r , and fit fraction asymmetries as an estimation of the systematic uncertainty.

Contributions to the experimental systematic uncertainties arise from our model of the background, the efficiency and the event selection. Our nominal fit fixes the coefficients of the background determined from a sideband region. To estimate the systematic uncertainty on this background shape, a fit is done with the coefficients allowed to float and constrained by the covariance matrix obtained from the background fit. Similarly, to estimate the systematic uncertainty on the efficiency parameters, we perform a fit with the coefficients of efficiency allowed to float constrained by their covariance matrix. To estimate the systematic uncertainty on MC simulation for the particle identification, a fit is done with new efficiency parameters obtained from the weighted MC sample by the efficiency ratios of data to MC depending on each particle's momentum. To estimate the event selection uncertainty, we

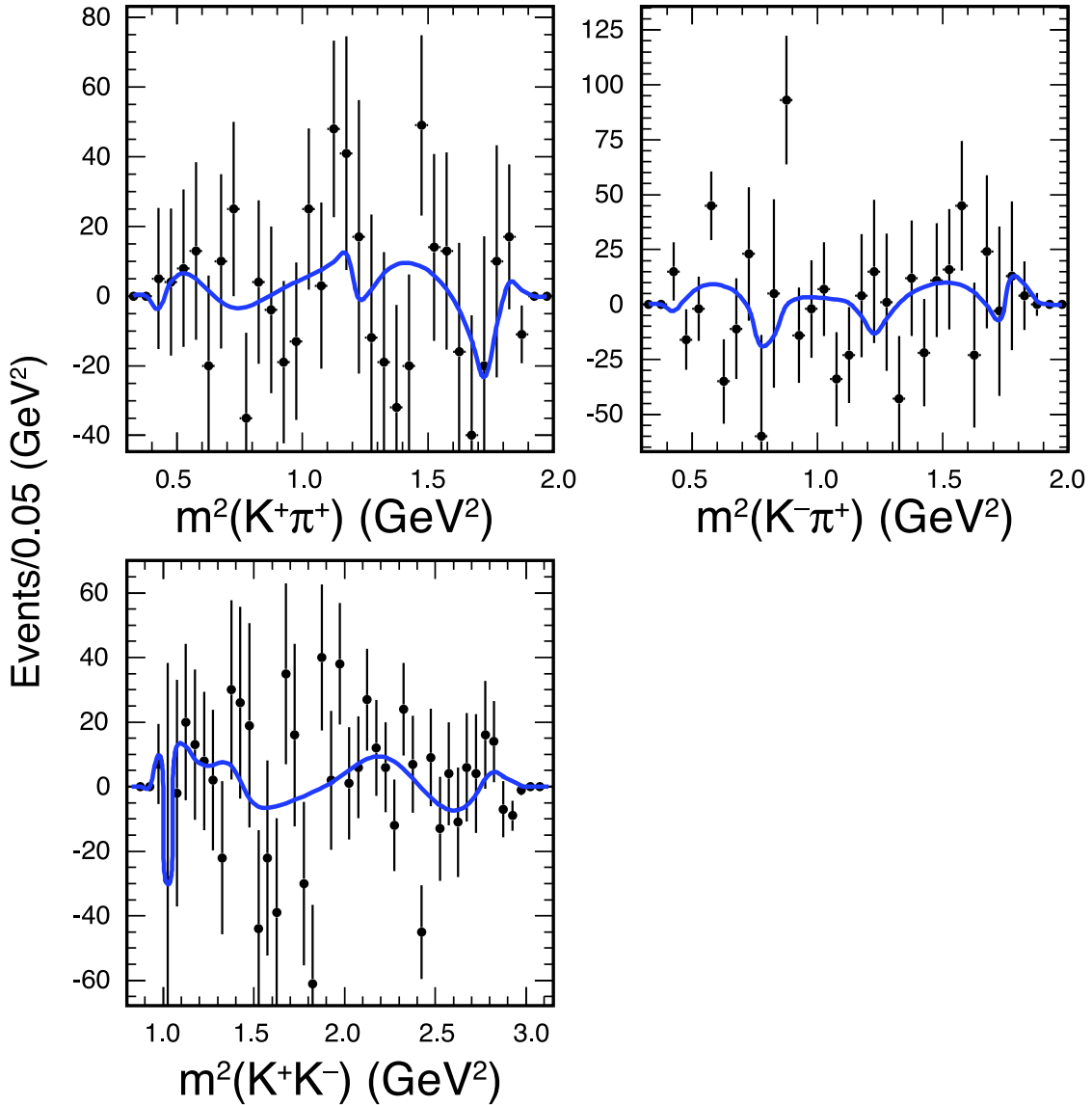


FIG. 4: The difference of the Dalitz-plot projections of data (points) and fit (line) between D^+ and D^- decays.

change the ΔE and m_{BC} selection criteria in the analysis. These variations to the standard fit are the largest contribution to our experimental systematic errors. In the CP asymmetry search, we take the background fractions and shapes to be the same for the D^+ and D^- samples. To estimate the uncertainty on the supposition, we perform a fit with the background determined separately.

The systematic error due to our choice of $D^+ \rightarrow K^+K^-\pi^+$ decay model is evaluated as follows. We change the standard values of the radial parameter in the Blatt-Weisskopf form factors [14] for the intermediate resonance decay vertex (1.5 GeV^{-1}) and the D^+ vertex (5 GeV^{-1}) both to 1 GeV^{-1} . Fits with constant width in the Breit-Wigner functions are considered. To compute the uncertainty arising from our choice of resonances included in the fit, we compare the result of our standard fit to a series of fits where each of the reso-

nances, $\overline{K}^*(1410)^0$, $f_0(980)$, $f_0(1370)$, $f_0(1500)$, $f_2(1270)$, $f_2'(1525)$, $a_0(980)^0$ and $a_2(1320)^0$, is included one at a time. These variations to the standard fit result in the largest contribution to systematic errors associated with our decay model. The masses and widths of the intermediate resonances are allowed to vary within their known uncertainties [15]. For fit C, we vary the parameters in the LASS amplitude within their uncertainties.

We take the maximum variation of the magnitudes, phases, and fit fractions, b_r/a_r , ϕ_r , and fit fraction asymmetries from the nominal fit compared to the results in this series of fits as a measure of the experimental systematic and decay-model systematic uncertainty. Table IV shows the systematic checks on the integrated CP asymmetry defined in Eq. (18). Apart from the sources discussed above, we also consider different models from fit A or C; the variations are small.

TABLE IV: Sources contributing to systematic uncertainties on the integrated CP asymmetry defined in Eq. (18).

Source	Variation (%)
Background shape	-0.01
Efficiency parameters	+0.02
Particle identification	+0.06
Event selection criteria	+0.18
Background (in)dependent fit	-0.52
Form factors	+0.21
Width parameterization	-0.15
Choice of resonances	+0.61 -0.33
Resonant masses and widths	+0.09 -0.08
Fit A	+0.07
Fit C	-0.15

We estimate the systematic uncertainty on the CP asymmetry defined in Eq. (4). The contributions from various identified sources are listed in Table V. The uncertainty due to selection criteria is estimated by doubling the ΔE signal window. We evaluate an uncertainty for the background shape by floating its parameters in the fit instead of fixing them from the values obtained from the ΔE sideband. We use the CP -conserved channels $D^+ \rightarrow K^- \pi^+ \pi^+$ and $D^0 \rightarrow K^- \pi^+ \pi^0$ as control modes to assign the systematic uncertainty on MC simulation due to possible efficiency difference on positive and negative charged kaons and pions.

TABLE V: Systematic uncertainties on the CP asymmetry defined in Eq. (4).

Source	Variation (%)
Selection criteria	± 0.25
Background shape	± 0.02
MC simulation	± 0.15
Total	± 0.29

In conclusion, we have analyzed the resonant substructure in $D^+ \rightarrow K^+ K^- \pi^+$ decay and searched for CP violation in the decay and its intermediate resonances. We measure the

overall CP asymmetry in $D^\pm \rightarrow K^+K^-\pi^\pm$ decays to be $(-0.03 \pm 0.84 \pm 0.29)\%$. The limit is more restrictive than the one found previously by *BABAR* [6]. We use five resonances and $K^-\pi^+$ S -wave states to model the Dalitz plot with results shown in Table I. The $K^-\pi^+$ S -wave can be equally well described by a coherent sum of $\overline{K}_0^*(1430)^0$ and nonresonant amplitude or $\overline{K}_0^*(1430)^0$ and $\kappa(800)$, or the LASS amplitude. Choosing the second model we measure the CP asymmetries for all submodes, shown in Table II and III. The measured CP asymmetries are consistent with the absence of CP violation. We find \mathcal{A}_{CP} defined in Eq. (18) to be $(-0.4 \pm 2.0_{-0.5-0.3}^{+0.2+0.6})\%$. The \mathcal{A}_{CP} is sensitive to an asymmetry in shape between the D^+ and D^- samples, but does not depend on their yields.

We gratefully acknowledge the effort of the CESR staff in providing us with excellent luminosity and running conditions. D. Cronin-Hennessy and A. Ryd thank the A.P. Sloan Foundation. This work was supported by the National Science Foundation, the U.S. Department of Energy, the Natural Sciences and Engineering Research Council of Canada, and the U.K. Science and Technology Facilities Council.

-
- [1] F. Buccella, M. Lusignoli, G. Mangano, G. Miele, A. Pugliese, and P. Santorelli, *Phys. Lett. B* **302**, 319 (1993); F. Buccella, M. Lusignoli, G. Miele, A. Pugliese, and P. Santorelli, *Phys. Rev. D* **51**, 3478 (1995); M. Golden and B. Grinstein, *Phys. Lett. B* **222**, 501 (1989).
 - [2] S. Bianco, F. L. Fabbri, D. Benson, and I. Bigi, *Riv. Nuovo Cimento* **26N7**, 1 (2003).
 - [3] Y. Grossman, A. L. Kagan, Y. Nir, *Phys. Rev. D* **75**, 036008 (2007).
 - [4] P. L. Frabetti *et al.* (E687 Collaboration), *Phys. Lett. B* **351**, 591 (1995).
 - [5] J. M. Link *et al.* (FOCUS Collaboration), *Phys. Lett. B* **648**, 156 (2007).
 - [6] B. Aubert *et al.* (*BABAR* Collaboration), *Phys. Rev. D* **71**, 091101(R) (2005).
 - [7] S. Dobbs *et al.* (CLEO Collaboration), *Phys. Rev. D* **76**, 112001 (2007).
 - [8] Y. Kubota *et al.*, *Nucl. Instrum. Methods Phys. Res., Sect. A* **320**, 66 (1992).
 - [9] D. Peterson *et al.*, *Nucl. Instrum. Methods Phys. Res., Sect. A* **478**, 142 (2002).
 - [10] M. Artuso *et al.*, *Nucl. Instrum. Methods Phys. Res., Sect. A* **554**, 147 (2005).
 - [11] T. Skwarnicki, Ph.D thesis, Institute for Nuclear Physics, Krakow, Poland (1986).
 - [12] H. Albrecht *et al.* (ARGUS Collaboration), *Phys. Lett. B* **229**, 304 (1989).
 - [13] S. Kopp *et al.* (CLEO Collaboration), *Phys. Rev. D* **63**, 092001 (2001).
 - [14] J. Blatt and V. Weisskopf, *Theoretical Nuclear Physics* (Wiley, New York, 1952).
 - [15] W.-M. Yao *et al.* (Particle Data Group), *Journal of Physics G* **33**, 1 (2006).
 - [16] M. Ablikim *et al.* (BES Collaboration), *Phys. Lett. B* **607**, 243 (2005).
 - [17] A. Abele *et al.* (Crystal Barrel Collaboration), *Phys. Rev. D* **57**, 3860 (1998).
 - [18] J. A. Oller, *Phys. Rev. D* **71**, 054030 (2005).
 - [19] D. Aston *et al.* (LASS Collaboration), *Nucl. Phys. B* **296**, 493 (1988).
 - [20] B. Aubert *et al.* (*BABAR* Collaboration), *Phys. Rev. D* **76**, 011102(R) (2007).
 - [21] D. M. Asner *et al.* (CLEO Collaboration), *Phys. Rev. D* **70**, 091101(R) (2004).